



HAL
open science

Mathematical modeling of complex forest ecosystems: impacts of deforestation

Guillaume Cantin, Nathalie Verdière

► **To cite this version:**

Guillaume Cantin, Nathalie Verdière. Mathematical modeling of complex forest ecosystems: impacts of deforestation. 2020. hal-02496187

HAL Id: hal-02496187

<https://hal.science/hal-02496187>

Preprint submitted on 2 Mar 2020

HAL is a multi-disciplinary open access archive for the deposit and dissemination of scientific research documents, whether they are published or not. The documents may come from teaching and research institutions in France or abroad, or from public or private research centers.

L'archive ouverte pluridisciplinaire **HAL**, est destinée au dépôt et à la diffusion de documents scientifiques de niveau recherche, publiés ou non, émanant des établissements d'enseignement et de recherche français ou étrangers, des laboratoires publics ou privés.

MATHEMATICAL MODELING OF COMPLEX FOREST ECOSYSTEMS: IMPACTS OF DEFORESTATION

Guillaume Cantin¹, Nathalie Verdière²

Abstract. We propose an innovative mathematical model for studying the dynamics of a complex network of forest ecosystems, in which two forest entities interact with each other through water exchanges. Our model reproduces a recently analyzed principle of constant precipitation quantity over densely forested areas. We perform a stability and bifurcation analysis and show that the distance separating two forest ecosystems can attract a part of the network to an extinction state. We incorporate a randomly generated perturbation modeling deforestation and investigate the effect of the level of deforestation on the equilibrium states of the network. We also exhibit a type of synchronization in the case of densely distributed forest ecosystems.

Keywords. Mathematical modeling, forest ecosystem, complex network, ecology, dynamical system.

§1. Introduction

In a context of international global warming, which is nowadays admitted at least by the scientific community, much emotion has been recently inspired by forest fires of unprecedented intensity, for instance in the Amazon forest, or very recently in south-east Australia [9]. Those forest fires are threatening the equilibrium of the climate, the diversity of wildlife and the lifeblood of our societies, thus it is an imperative to better understand the mechanisms which lead to the risk of forest fires, so as to fight and overcome this scourge. Anthropogenic cause of those catastrophic events are already observed [1] and analyzed as a tipping point [20]. Numerous studies of forest fires have been proposed (see for instance [18], [22], [24]) and it is recognized that the dynamics of forest ecosystems enjoy the characteristics of complexity (see [12] for a survey and references therein). As a key ingredient of that complexity, deforestation is studied in [19], and its impact on wildlife is analyzed in [25] for instance. Recently, much attention has been paid on the role of water evaporation over the forested areas in order to describe a drought process which can exacerbate the fire risk. The *biotic pump* mechanism has been studied in [17], where it is remarked that over extensive natural forests, precipitation does not depend on the distance from the ocean along several thousand kilometers. Furthermore, deforestation, whatever its cause may be, is suspected by the same authors to induce a cascade of climatic effects, including disruption of the biotic pump [6].

Our aim in this article is to propose an innovative mathematical model for understanding the dynamics of complex forest ecosystems, by taking into account this biotic pump mechanism. Many works have certainly been devoted to modeling forest ecosystems. For instance, age or size structure mathematical models have been analyzed in [7]; multi-species models have been studied in [13]; partial differential equations models are proposed and studied in [15], [16]; cellular automata models are also studied, for instance in [2], [10]. However, at our knowledge, none of those models incorporates the effect of water evaporation over forest areas, although this mechanism is well-known for several decades [11], [27]. It is our purpose in this work to fill this void. We focus on forest areas of heterogeneous structure, and propose an original mathematical model which takes the form of a complex network of dynamical systems. Hence, the construction of this innovative mathematical model represents a novel contribution to the study of complex forest ecosystems. Complex networks of dynamical systems have proved their great interest in various research fields such as behavioral models, neural networks or epidemiological networks (see for instance [4], [5], [8]). Here, we use this complex network framework for studying forest ecosystems, by modeling the dynamics of each forest entity by an age structure

¹Laboratoire de Mathématiques Appliquées, FR-CNRS-3335, 25, rue Philippe Lebon, 76063 Le Havre Normandie, France. E-mail: guillaumecantin@mail.com

²Laboratoire de Mathématiques Appliquées, FR-CNRS-3335, 25, rue Philippe Lebon, 76063 Le Havre Normandie, France. E-mail: nathalie.verdiere@univ-lehavre.fr

model, proposed by Antonovsky & Korzukhin [3], and by modeling the interactions between two forest entities with each other through water resource exchanges.

Our complex network model for analyzing the dynamics of forest ecosystems leads to the study of a complex dynamical system, which we study using techniques of stability analysis and bifurcation analysis (see for instance [14] or [23]). We first show that our model is able to reproduce the principle of uniform precipitation quantity over densely forested areas, by comparing our biotic pump modeling with real world data. Then we focus on the study of a two forests network and establish the list and the nature of equilibrium states. We prove an important pattern, which is recovered in the general case of a multiple forests network: if the distance separating two forests ecosystems increases and overcomes a threshold, then the one which is located far from the coastline is likely to converge to the trivial equilibrium, which corresponds to a vanishing state of the ecosystem. This pattern is in concordance with the precipitation exponential decreasing principle remarked in [17]. Furthermore, we improve our complex network model by incorporating a randomly generated perturbation which models deforestation. We perform a sensitivity analysis of the resulting system and show the impact of the level of deforestation of the equilibrium states of the complex network of forest ecosystems. We also analyze the effect of the locations of deforested areas in the network and prove that a low level of deforestation can lead the whole network to an extinction state. In parallel, we exhibit a type of synchronization in the case of densely distributed forest ecosystems networks.

Our paper is organized as follows. In the next section, we present the main ingredients of our complex network model, namely the Antonovsky & Korzukhin age structure model, and the biotic pump mechanism. We show that the resulting Cauchy problem is well-posed and admits relevant solutions, that is, positive and bounded solutions. In section 3, we present the stability and bifurcation analysis of a simple two forests network, in order to identify the main trends of the model. In the final section, we improve the initial complex network problem by incorporating a randomly generated perturbation and present numerical simulations of the complete model.

§2. Setting of the problem

In this section, we present the age structure mathematical model proposed in [3] by Antonovsky & Korzukhin for studying the dynamics of a one-species forest ecosystem. Then we propose an original model of the biotic pump mechanism and we construct a novel mathematical model which takes the form of a complex network of dynamical systems.

2.1. Antonovsky & Korzukhin model

Let us consider a forest ecosystem and assume that it can be assimilated to a one-species ecosystem; we divide the population of trees of that forest ecosystem into two sub-populations, distinguishing the young trees and the old trees. We denote by $x(t)$ and $y(t)$ the densities of young trees and old trees respectively, at time t . Those densities are expressed by number per unit of surface (thousands per hectare for example), and time t is expressed in years. Antonovsky & Korzukhin [3] have proposed a simplified mathematical model for studying the dynamics of such a forest ecosystem. Their model is given by the following system of two ordinary differential equations:

$$\begin{cases} \dot{x} = \rho y - \gamma(y)x - fx \\ \dot{y} = fx - hy, \end{cases} \quad (1)$$

where the parameters ρ , f and h are positive real coefficients. The parameter ρ in the first equation of system (1) models the fertility of the species; h and f are mortality rate of old trees and aging rate of young trees respectively; the function $\gamma(y)$ corresponds to the mortality rate of young trees; it is usually defined by a quadratic expression of the form

$$\gamma(y) = a(y - b)^2 + c, \quad (2)$$

where a , b and c are positive coefficients. The equation (2) takes into account the competition between young and old trees for life resources, including water and light; this quadratic expression guarantees

convexity, thus a minimum for $\gamma(y)$ which means that there exists an optimal value of old trees density under which the development of young trees goes on most successfully.

The dynamics and bifurcation analysis of Antonovsky & Korzukhin model is presented in [3]. It is shown that there exists three parameter regimes. The first parameter regime leads to the existence and uniqueness of the trivial equilibrium $(0, 0)$, which models the extinction of the ecosystem. The second parameter regime guarantees the coexistence of three equilibrium states: the trivial equilibrium $(0, 0)$, a saddle point (\bar{x}, \bar{y}) and an attractive node (x^*, y^*) which is locally asymptotically stable and models a stationary state with constant age class densities. The third parameter regime yields the existence and uniqueness of a non-trivial attractive node (x^*, y^*) . Figure 1 shows a phase portrait of system (1) corresponding to the second parameter regime; the trivial equilibrium attracts the orbits to an extinction state of the ecosystem, whereas the non-trivial stable node attracts the orbits to a good health state of the ecosystem. Their basins of attraction are separated by the stable manifold of the saddle-point.

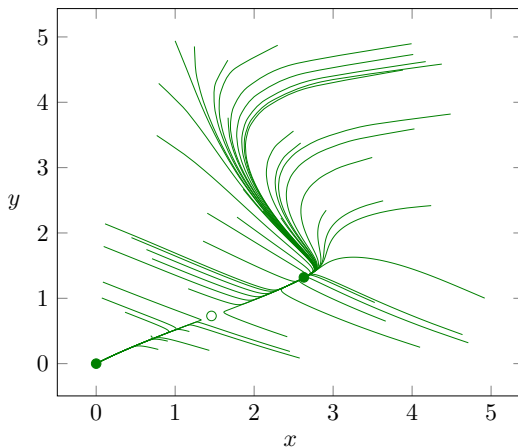


Figure 1: Phase portrait of Antonovsky & Korzukhin model (1) obtained for $\rho = 4.2$, $f = 1$, $h = 2$, $a = 1$, $b = 1$, $c = 1$, showing the coexistence of three equilibrium states: the trivial equilibrium $(0, 0)$, a saddle point (\bar{x}, \bar{y}) and an attractive node (x^*, y^*) which is locally asymptotically stable and models a stationary state with constant age class densities.

Antonovsky & Korzukhin model has been calibrated in order to fit with data of real forest ecosystems; it has also been considered as a basis for refined models of forest ecosystems, studying interaction with pests [3], or diffusion of seeds [15] for instance.

2.2. Mathematical modeling of the biotic pump mechanism

We recall that our aim is to propose a novel mathematical model for studying the dynamics of a complex network of forest ecosystems, in which two forests interact with each other through exchanges of water resource. In this paragraph, we show how to model the biotic pump mechanism which describes the consumption and the production of water by a given forest ecosystem. To this end, we consider a simplified complex network of forest ecosystems, distributed along a line stemming from an ocean and directed towards a continental area. We assume that the region is occupied by a finite number of forest ecosystems, the first one being located nearby the coastline, as depicted in Figure 2. Furthermore, we assume that the dominant winds bring the water evaporated over the maritime zone towards the continental area.

We aim to reproduce two principles which are discussed in [17]: on the one hand, over non-forested areas, precipitation decreases exponentially with distance from the ocean; on the other hand, over extensive natural forests, precipitation does not depend on the distance from the ocean along several thousand kilometers. A qualitative comparison of our model with precipitation data of the Amazon basin will be presented below.

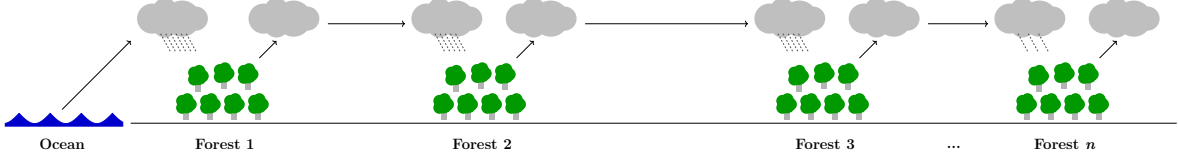


Figure 2: Schema of a simplified complex network of forest ecosystems, distributed along a line stemming from an ocean and directed towards a continental area. Two forests interact with each other through exchanges of water resource.

Once again, we divide the population of trees into two sub-populations x and y corresponding to young and old trees respectively. In a complex network of n forest ecosystems, we denote by (x_i, y_i) the sub-populations of young and old trees of i -th forest respectively, and we denote by S_i the surface of i -th forest. For each $i \in \{1, \dots, n-1\}$, let $w_{i+1}(x_1, y_1, \dots, x_i, y_i)$ denote the average in time water quantity received by the $(i+1)$ -th forest ecosystem of the complex network. For the first forest which is located nearby the ocean, at $d = 0$, we set

$$w_1 = P_0, \quad (3)$$

where P_0 is a non-negative coefficient which models the average water quantity available for the first forest ecosystem, evaporated over the maritime zone. Furthermore, we assume that the first forest produces by evaporation a quantity of water $B(x_1, y_1)$, which increases with x_1 and y_1 . We propose to model this quantity by a linear function of the form

$$B(x_1, y_1) = \beta_1(S_1)x_1 + \beta_2(S_1)y_1, \quad (4)$$

where $\beta_1(S_1)$ and $\beta_2(S_1)$ are non-negative coefficients which may depend on the surface S_1 of the first forest.

Next, for the second forest ecosystem, which is located at a distance equal to d_1 from the first forest, we assume that the quantity of water $P_0 + B(x_1, y_1)$, which is available at $d = 0$, decreases exponentially with d_1 (see [17]), thus we set

$$w_2(x_1, y_1) = [P_0 + B(x_1, y_1)] \exp\left\{\frac{-d_1}{l}\right\}, \quad (5)$$

where l is a positive normalization coefficient which can be determined from the size of the forested area (see [17]).

Now, let us denote by d_i the distance separating the i -th forest from the $(i+1)$ -th forest. We assume that the water quantity received by the $(i+1)$ -th forest ecosystem corresponds to the sums of the water quantities produced by the previous forests, weighted by a decreasing exponential factor which models the distance browsed by those water quantities. Hence we set

$$\begin{aligned} w_{i+1}(x_1, y_1, \dots, x_i, y_i) &= [P_0 + B(x_1, y_1)] \exp\left\{\frac{-(d_1 + \dots + d_i)}{l}\right\} \\ &+ B(x_2, y_2) \exp\left\{\frac{-(d_2 + \dots + d_i)}{l}\right\} + \dots + B(x_i, y_i) \exp\left\{\frac{-d_i}{l}\right\}, \end{aligned} \quad (6)$$

for each $1 \leq i \leq n-1$, where $B(x_i, y_i)$ corresponds to the quantity of water evaporated over i -th forest, given by

$$B(x_i, y_i) = \beta_1(S_i)x_i + \beta_2(S_i)y_i, \quad (7)$$

with S_i denoting the surface of i -th forest. In the rest of the paper, in order to simplify our model, we will assume that each forest ecosystem admits the same surface, that is, $S_i = S_j$ for all i and j such that $1 \leq i \leq n$ and $1 \leq j \leq n$. Consequently, the parameters β_1 and β_2 involved in equation (7) will admit the same value for each forest ecosystem. It is worth emphasizing that the quantity of water w_i received by the i -th forest ecosystem depends on the densities of young and old trees $x_1, y_1, x_2, y_2, \dots, x_{i-1}, y_{i-1}$ of the previous forest ecosystems. Those exchanges of water quantities can be modeled by an oriented graph, as depicted in Figure 3. In this figure, the blue vertex models the maritime zone, and the green vertices model the forest ecosystems. Each oriented edge models an exchange of water quantity.

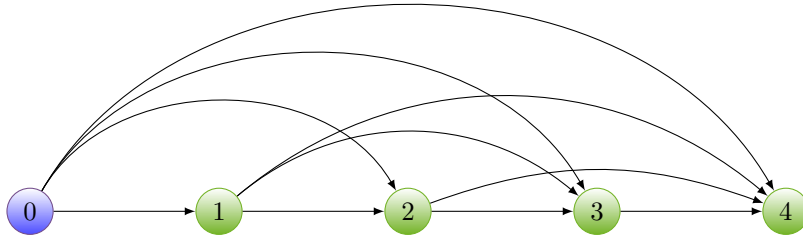


Figure 3: Oriented graph corresponding to a simplified complex network of forest ecosystems. The blue vertex models the maritime zone, and the green vertices model the forest ecosystems. Each oriented edge models an exchange of water quantity.

2.3. Penalty induced by the biotic pump mechanism

Finally, we suppose that the quantity of water which is received by each forest ecosystem determines a positive or a negative effect on this ecosystem. We assume that a low quantity of water w induces a penalty which in turn implies a decreasing effect on the densities of trees. At the opposite, we assume that if the quantity of water w overcomes a certain threshold w_0 , then the densities of trees are augmented by a positive effect. In order to model this mechanism, we introduce the penalty function $\alpha(w)$ defined by

$$\alpha(w) = \alpha_0 \left(1 - \frac{w}{w_0} \right), \quad (8)$$

where α_0 is a negative coefficient and w_0 a positive coefficient (see figure 4).

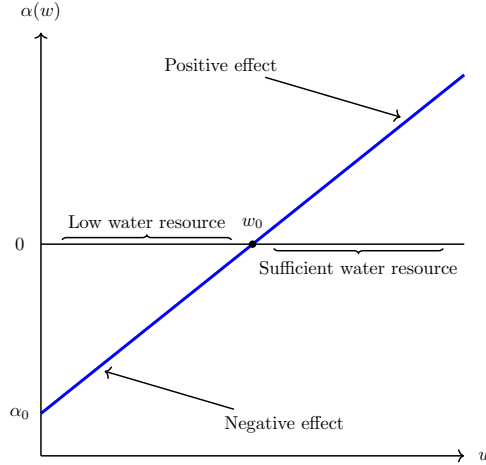


Figure 4: Penalty function $\alpha(w)$. A low quantity of water w induces a penalty which in turn implies a decreasing effect on the densities of trees. If the quantity of water w overcomes a certain threshold w_0 , then the densities of trees are augmented by a positive effect.

We introduce the notations

$$\alpha_1 = \alpha(w_1), \quad \alpha_i(x_1, y_1, \dots, x_{i-1}, y_{i-1}) = \alpha(w_i(x_1, y_1, \dots, x_{i-1}, y_{i-1})), \quad (9)$$

for $2 \leq i \leq n$, where $w_i(x_1, y_1, \dots, x_{i-1}, y_{i-1})$ represents the quantity of water received by the i -th forest, given by equation (6). As for the quantity of water w_i received by the i -th forest ecosystem, the coefficient α_i depends on the densities of young and old trees $x_1, y_1, x_2, y_2, \dots, x_{i-1}, y_{i-1}$ of the previous forest ecosystems.

2.4. Complex network of forest ecosystems

Now we are ready to present the construction of a mathematical model for studying the dynamics of a complex network of forest ecosystems. We consider as before a simplified distribution of n forest ecosystems along a directed line ($n \geq 2$), as depicted in Figure 2 and represented in Figure 3. We denote again by x_i and y_i the densities of young and old trees respectively, in the i -th forest ecosystem ($1 \leq i \leq n$). We recall that x_i and y_i are expressed by numbers per unit of surface, time t is expressed in years, and we assume that each forest ecosystem has the same surface. Next, we model the state of each forest ecosystem by an instance of Antonovsky & Korzukhin model given by system (1) and we consider the water interactions between those forest ecosystems by incorporating the penalty functions α_i , $1 \leq i \leq n$, defined by (6), (7) and (9) into the state equations of x_i and y_i . Thus we consider the following complex network problem:

$$\begin{cases} \dot{x}_1 = \rho y_1 - \gamma(y_1)x_1 - f x_1 + a_1 \alpha_1 x_1 \\ \dot{y}_1 = f x_1 - h y_1 + a_2 \alpha_1 y_1 \\ \dot{x}_2 = \rho y_2 - \gamma(y_2)x_2 - f x_2 + a_1 \alpha_2(x_1, y_1)x_2 \\ \dot{y}_2 = f x_2 - h y_2 + a_2 \alpha_2(x_1, y_1)y_2 \\ \vdots \\ \dot{x}_n = \rho y_n - \gamma(y_n)x_n - f x_n + a_1 \alpha_n(x_1, y_1, \dots, x_{n-1}, y_{n-1})x_n \\ \dot{y}_n = f x_n - h y_n + a_2 \alpha_n(x_1, y_1, \dots, x_{n-1}, y_{n-1})y_n, \end{cases} \quad (10)$$

where ρ , f and h are positive real coefficients, γ is given by (2); a_1 , a_2 are non-negative weights of the biotic pump mechanism which model the sensitivities to the water resource of young and old trees respectively. We shall assume that young trees are more sensitive to a variation of the water resource, which means that $a_2 < a_1$. The significances of the parameters are gathered in Table 1.

Table 1: Parameters involved in the biotic pump mechanism determined by equations (6), (7), (9) and in the complex network of forest ecosystems (10), with their significance and unit.

Parameter	Significance	Unit
ρ	fertility of the species	year ⁻¹
$\gamma(y)$	mortality rate of young trees	year ⁻¹
f	aging rate	year ⁻¹
h	mortality rate of old trees	year ⁻¹
a_1	biotic pump weight of young trees	dimensionless
a_2	biotic pump weight of old trees	dimensionless
d_i	distance separating forests i and $i + 1$ ($1 \leq i \leq n - 1$)	km
α_i	penalty rate of i -th forest ($1 \leq i \leq n$)	year ⁻¹
w_i	water quantity received by i -th forest ($1 \leq i \leq n$)	mm \times ha ⁻¹ \times year ⁻¹
S_i	surface of i -th forest ($1 \leq i \leq n$)	ha
β_1	water evaporation coefficient of young trees	mm \times year ⁻¹
β_2	water evaporation coefficient of old trees	mm \times year ⁻¹

The complex network (10) problem enjoys a master-slave structure, since (x_1, y_1) can be determined independently of the rest of the system, whereas (x_2, y_2) depends on (x_1, y_1) and more generally, (x_i, y_i) depends on $(x_1, y_1, \dots, x_{i-1}, y_{i-1})$. This master-slave structure is related to the topology of the oriented graph which underlies the complex network problem (see Figure 3). Furthermore, the complex network problem (10) admits two non-linearities, which are firstly stored in the mortality

terms $-\gamma(y_i)x_i$ and secondly contained in the interaction terms $a_1\alpha_i(x_1, y_1, \dots, x_{i-1}, y_{i-1})x_i$ and $a_2\alpha_i(x_1, y_1, \dots, x_{i-1}, y_{i-1})y_i$.

Remark 1. We emphasize that the interaction terms of the complex network model (10) model exchanges of water resource; those couplings, which are of quadratic type, obviously do not imply migrations of biological individuals from one forest ecosystem to another. This differentiates our model from numerous complex networks where the couplings, which are of linear type, correspond to displacements of individuals (see the models studied in [4] or in [5] for example).

2.5. Non-negativity and boundedness of solutions of the complex network model

The complex network model (10) can be rewritten in a short form

$$\dot{X} = F_n(X), \quad (11)$$

where $X = (x_1, y_1, \dots, x_n, y_n)^T$ and $F_n(X) = (f_1(X), g_1(X), \dots, f_n(X), g_n(X))^T$ with

$$\begin{aligned} f_i(X) &= \rho y_i - \gamma(y_i)x_i - f x_i + a_1\alpha_i(x_1, y_1, \dots, x_{i-1}, y_{i-1})x_i, \\ g_i(X) &= f x_i - h y_i + a_2\alpha_i(x_1, y_1, \dots, x_{i-1}, y_{i-1})y_i, \end{aligned} \quad (12)$$

for each $i \in \{1, \dots, n\}$. Note that f_i and g_i are polynomials of cubic order in X .

The two following theorems guarantee that the complex network problem (10) admits relevant solutions, that is, global solutions with non-negative components.

Theorem 1. For any initial condition X_0 in $(\mathbb{R}^+)^{2n}$, the Cauchy problem determined by (10) and $X(0) = X_0$ admits a unique local in time solution $X(t, X_0)$ defined on a time interval $[0, T]$ with $T > 0$, whose components are non-negative on $[0, T]$.

Proof. Since the operators f_i and g_i defined by (12) are polynomials, the existence and uniqueness of a local in time solution stemming from any initial condition X_0 in \mathbb{R}^{2n} directly follows from general results of the theory of ordinary equations (see [23] for instance).

Next, it is seen that the operator $F_n = (f_1, g_1, \dots, f_n, g_n)^T$ defined in \mathbb{R}^{2n} by (11) is quasi-positive, which means that it satisfies the property

$$f_j(u_1, \dots, u_{i-1}, 0, u_{i+1}, \dots, u_{2n}) \geq 0, \quad g_j(u_1, \dots, u_{i-1}, 0, u_{i+1}, \dots, u_{2n}) \geq 0,$$

for all $u = (u_1, \dots, u_{2n}) \in (\mathbb{R}^+)^{2n}$, $i \in \{1, \dots, 2n\}$ and $j \in \{1, \dots, n\}$. By virtue of Proposition A.17 in [26], it follows that the components of any solution $X(t, X_0)$ stemming from X_0 in $(\mathbb{R}^+)^{2n}$ remain non-negative in future time. \square

Theorem 2. Assume that a_2 is sufficiently small. Then one can find positive constants $A_1, B_1, \dots, A_n, B_n$ such that the region

$$\mathcal{R} = \prod_{i=1}^n [0, A_i] \times [0, B_i]$$

is positively invariant for the flow induced by the complex network problem (10), which means that $X_0 \in \mathcal{R}$ implies $X(t, X_0) \in \mathcal{R}$ for all $t \in [0, T]$.

Proof. Let $X(t, X_0) = (x_1(t), y_1(t), \dots, x_n(t), y_n(t))$ denote the solution of system (10) stemming from X_0 in \mathcal{R} . Using the master-slave structure of system (10), we first determine positive constants A_1 and B_1 so that the product set $[0, A_1] \times [0, B_1]$ is positively invariant for $(x_1(t), y_1(t))$. A sufficient condition is that the vector field $F_n(X)$ points into the interior of the region when evaluated on its boundary (see [21] for instance). This sufficient condition can be written

$$\rho B_1 - \gamma(B_1)A_1 - f A_1 + a_1\alpha_1 A_1 < 0, \quad (13)$$

$$f A_1 - (h - a_2\alpha_1)B_1 < 0. \quad (14)$$

We fix $A_1 > 0$. Parameter a_2 can be chosen small enough so that $h > a_2\alpha_1$, so one can find a positive constant B_1 such that condition (14) is fulfilled. Furthermore, the function $\gamma(y)$ defined by (2) is polynomial of order 2; this guarantees that B_1 can be chosen large enough (increase B_1 if necessary) in order to guaranty that condition (13) is fulfilled simultaneously.

Next we determine positive constants A_2, B_2 so that $[0, A_1] \times [0, B_1] \times [0, A_2] \times [0, B_2]$ is positively invariant for $(x_1(t), y_1(t), x_2(t), y_2(t))$. Since A_1 and B_1 have already been chosen, a sufficient condition is

$$\rho B_2 - \gamma(B_2)A_2 - fA_2 + a_1\alpha_2(A_1, B_1)A_2 < 0, \quad fA_2 - (h - a_2\alpha_2(A_1, B_1))B_2 < 0.$$

As before, we fix $A_2 > 0$ and we determine B_2 using the inequality $h > a_2\alpha_2(A_1, B_1)$, which is fulfilled for a_2 sufficiently small, and the fact that $\gamma(y)$ is polynomial of order 2.

Finally, we can repeat those arguments a finite number of times in order to determine positive constants A_i and B_i for $2 \leq i \leq n$. \square

Remark 2. *The requirement on parameter a_2 to be small enough is sufficient in order to guaranty that $a_2\alpha_i(A_1, B_1, \dots, A_{i-1}, B_{i-1}) < h$ for each $i \in \{1, \dots, n\}$. This assumption corresponds to the situation when old trees y_i are less sensitive than young trees x_i to a variation of available resource in water, which is relevant from the biological point of view.*

Theorems 1 and 2 imply that the complex network problem (10) admits non-negative and bounded solutions, thus global in time solutions, which is a first condition to be satisfied for the validation of the model.

2.6. Qualitative comparison of our model with precipitation data of the Amazon basin

Let us briefly show how our model can fit with real collected data. We compare in Figure 5 a plot of precipitation data of the Amazon basin (green squares), and the results of a numerical simulation of our model (red dots). The data (collected from LBA-HydroNet Collection, Climatological Dataset and provided by the Water Systems Analysis Group, University of New Hampshire) were interpolated as monthly time series data for 1960-1990 from Webber and Willmott's station-record archive [28]. The spatial resolution of this data is 0.5 degrees as the original. We show the average precipitation over the Amazon basin at fix longitude 9.75 South, with variable latitude from 62 West to 72 West, which roughly represents 1000 km. Those data fit with the second principle mentioned above, which claims that over extensive natural forests, precipitation does not depend on the distance from the ocean.

In parallel, we have performed a numerical simulation of our complex network model (10) with the following parameters values: $n = 150$, $\rho = 4.2$, $a = 1$, $b = 1$, $c = 1$, $w_0 = 1.8$, $\alpha_0 = -0.03$, $a_1 = 0.7$, $a_2 = 0.9$, $f = 1$, $h = 2$, $l = 800$, $P_0 = 0.65$, $D = 1000$, $d = D/(n - 1)$, $\beta_1 = 0.003$, $\beta_2 = 0.004$. The large value of n reproduces a densely forested area.

This comparison highlights that our model is able to reproduce a situation where the quantity of water resource received by a forest ecosystem is almost constant with respect to the distance from the ocean. However, the precise numerical calibration of the parameters of our model is not discussed further in this article, and will be presented in a separate paper, using techniques of identifiability [29].

§3. Stability analysis and bifurcation analysis of a two forests network

In this section, we present a qualitative analysis of a two forests network, in which two forest ecosystems are separated by a distance d_1 . We focus on the effect of a variation of d_1 on the dynamics and bifurcations of the complex network and prove that an increase of d_1 makes non-trivial equilibrium states vanish.

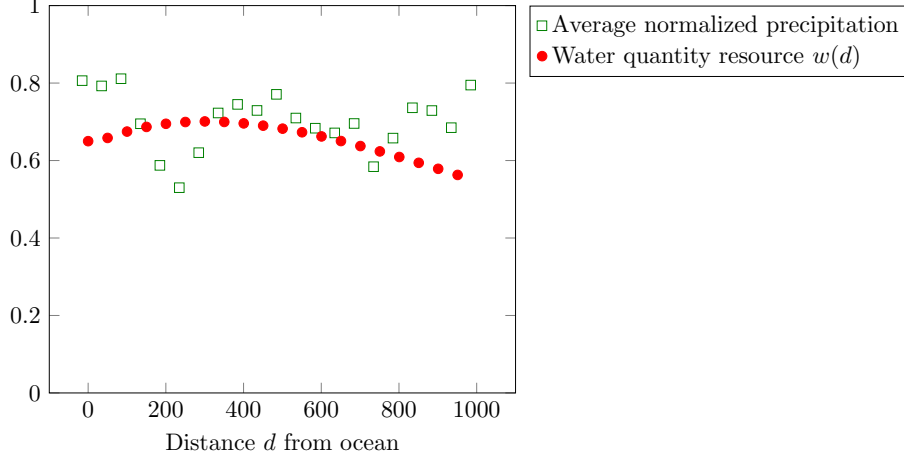


Figure 5: Qualitative comparison of precipitation data of the Amazon basin (green squares) with results of a numerical simulation of our complex network model (red dots). Over extensive natural forests, precipitation does not depend on the distance from the ocean.

3.1. Equations of a two forests network

Let us consider two forest ecosystems separated by a distance d_1 and assume as previously that the first ecosystem is located nearby the coastline. Such a two forests network is modeled by the following system of ordinary differential equations:

$$\begin{cases} \dot{x}_1 = \rho y_1 - \gamma(y_1)x_1 - f x_1 + a_1 \alpha_1 x_1 \\ \dot{y}_1 = f x_1 - h y_1 + a_2 \alpha_1 y_1 \\ \dot{x}_2 = \rho y_2 - \gamma(y_2)x_2 - f x_2 + a_1 \alpha_2(x_1, y_1)x_2 \\ \dot{y}_2 = f x_2 - h y_2 + a_2 \alpha_2(x_1, y_1)y_2. \end{cases} \quad (15)$$

This system can also be written in a short form

$$\dot{X} = F_2(X), \quad X = (x_1, y_1, x_2, y_2)^T.$$

Note that the parameter α_2 depends on (x_1, y_1) , as shown in equation (9).

3.2. Steady states and their stability

First, we present the research of the steady states and their stability of the two forests network problem given by (15). In order to avoid unreadable expressions of the steady states, we simplify the system by setting $a_2 = 0$. This assumption is reasonable, since the coefficient a_2 weights the penalties $\alpha_1 y_1$ and $\alpha_2(x_1, y_1)y_2$ on water resource for old trees, which is assumed to be negligible with respect to the penalties $\alpha_1 x_1$ and $\alpha_2(x_1, y_1)x_2$ on water resource for young trees.

As mentioned previously, the two forests network problem (15) admits a master-slave structure. Thus we begin with the research of the equilibrium states of the first forest ecosystem. Let us introduce the notation

$$k = \frac{1}{a} \left(\frac{\rho f}{h} + a_1 \alpha_1 - f - c \right).$$

Proposition 1. *Assume that $a_2 = 0$. If $k \geq 0$, then the equilibrium states of the sub-system given by the two first equations of problem (15) are given by*

$$e_1 = (0, 0), \quad e_2 = (\bar{x}_1, \bar{y}_1) = \left(\frac{h}{f}(b - \sqrt{k}), b - \sqrt{k} \right), \quad e_3 = (x_1^*, y_1^*) = \left(\frac{h}{f}(b + \sqrt{k}), b + \sqrt{k} \right).$$

If $k < 0$, then the sub-system given by the two first equations of problem (15) admits the trivial equilibrium $(0, 0)$ as a unique equilibrium state.

Proof. The research of the equilibrium states of the sub-system given by the two first equations of problem (15) leads to

$$\rho y_1 - \gamma(y_1)x_1 - f x_1 + a_1 \alpha_1 x_1 = 0, \quad f x_1 = h y_1.$$

Substituting $x_1 = \frac{h}{f} y_1$ into the first equation yields

$$y_1 \left(\rho - \gamma(y_1) \frac{h}{f} - h - a_1 \alpha_1 \frac{h}{f} \right) = 0,$$

thus $y_1 = 0$ or $\gamma(y_1) = \frac{\rho f}{h} - f + a_1 \alpha_1 = 0$, the latter equation being equivalent to

$$(y_1 - b)^2 = \frac{1}{a} \left(\frac{\rho f}{h} - f + a_1 \alpha_1 - c \right).$$

□

Next, we introduce the notations

$$\begin{aligned} \delta_0 &= \frac{-\alpha_0 a_1}{a w_0} (P_0 e^{-d_1/l} - P_0), & k_0 &= k + \delta_0, \\ \bar{\delta} &= \frac{-\alpha_0 a_1}{a w_0} [(P_0 + B(\bar{x}_1, \bar{y}_1)) e^{-d_1/l} - P_0], & \bar{k} &= k + \bar{\delta}, \\ \delta^* &= \frac{-\alpha_0 a_1}{a w_0} [(P_0 + B(x_1^*, y_1^*)) e^{-d_1/l} - P_0], & k^* &= k + \delta^*. \end{aligned} \quad (16)$$

It is easily seen that

$$\delta_0 \leq \bar{\delta} \leq \delta^*.$$

We recall that the coefficient α_0 is negative and we emphasize that the parameters δ_0 , $\bar{\delta}$ and δ^* can be negative, for instance if d_1 is large enough.

Theorem 3. *Assume that $a_2 = 0$, $k > 0$ and $b > \sqrt{k}$. Then the two-forests problem (15) admits at most 9 equilibrium points E_i , $1 \leq i \leq 9$, depending on the signs of k_0 , \bar{k} and k^* . The coordinates of those equilibrium points are given in Table 2. Furthermore, E_1 , E_2 and E_8 are attractive nodes and thus are locally asymptotically stable; E_3 , E_4 , E_5 and E_6 are saddle-points and thus are unstable; if $k^* < b^2$, then E_7 is an attractive node and E_9 is a saddle-point; if $k^* > b^2$, then E_9 is an attractive node and E_7 is a saddle-point.*

Proof. The research of the equilibrium states leads to the equations

$$x_2 = \frac{h}{f} y_2, \quad y_2 \left(\rho - \frac{h}{f} \gamma(y_2) - h + a_1 \frac{h}{f} \alpha_2(x_1, y_1) \right) = 0.$$

For any value of (x_1, y_1) , $(x_2, y_2) = (0, 0)$ fulfills the latter equations, which leads to the equilibrium points E_1 , E_4 and E_7 .

If $y_2 \neq 0$, we obtain

$$(y_2 - b)^2 = k + \frac{a_1}{a} (\alpha_2(x_1, y_1) - \alpha_1).$$

If $(x_1, y_1) = (0, 0)$, then $\alpha_2(x_1, y_1) = \alpha_2(0, 0)$ thus $\frac{a_1}{a} (\alpha_2(x_1, y_1) - \alpha_1) = \delta_0$, where δ_0 is defined in (16). It follows that

$$y_2 = b \pm \sqrt{k_0}, \quad x_2 = \frac{h}{f} y_2,$$

under the condition $k_0 \geq 0$, which corresponds to the equilibrium points E_2 and E_3 . Similarly, the case $(x_1, y_1) = (\bar{x}_1, \bar{y}_1)$ leads to the equilibrium points E_5 and E_6 which exist under the condition

Table 2: Steady states of the two forests network problem (15). The numbers of positive and negative eigenvalues of the jacobian matrix evaluated at the equilibrium points are denoted by n^+ and n^- respectively.

Equilibrium point	Nature	n^-	n^+
$E_1 = (0, 0, 0, 0)$	Attractive node	4	0
$E_2 = \left(0, 0, \frac{h}{f}(b + \sqrt{k_0}), b + \sqrt{k_0}\right)$	Attractive node	4	0
$E_3 = \left(0, 0, \frac{h}{f}(b - \sqrt{k_0}), b - \sqrt{k_0}\right)$	Saddle-point	3	1
$E_4 = (\bar{x}_1, \bar{y}_1, 0, 0)$	Saddle-point	≤ 3	≥ 1
$E_5 = \left(\bar{x}_1, \bar{y}_1, \frac{h}{f}(b + \sqrt{\bar{k}}), b + \sqrt{\bar{k}}\right)$	Saddle-point	≤ 3	≥ 1
$E_6 = \left(\bar{x}_1, \bar{y}_1, \frac{h}{f}(b - \sqrt{\bar{k}}), b - \sqrt{\bar{k}}\right)$	Saddle-point	≤ 3	≥ 1
$E_7 = (\bar{x}_1, \bar{y}_1, 0, 0)$			
If $k^* < b^2$:	Attractive node	4	0
If $k^* > b^2$:	Saddle-point	3	1
$E_8 = \left(x_1^*, y_1^*, \frac{h}{f}(b + \sqrt{k^*}), b + \sqrt{k^*}\right)$	Attractive node	4	0
$E_9 = \left(x_1^*, y_1^*, \frac{h}{f}(b - \sqrt{k^*}), b - \sqrt{k^*}\right)$			
If $k^* < b^2$:	Saddle-point	3	1
If $k^* > b^2$:	Attractive node	4	0

$\bar{k} \geq 0$, whereas the case $(x_1, y_1) = (x_1^*, y_1^*)$ leads to the equilibrium points E_8 and E_9 which exist under the condition $k^* \geq 0$.

Next, we determine the nature of the equilibrium points by examining the signs of the eigenvalues of the jacobian matrix evaluated at those equilibrium points. The jacobian matrix of system (15) reads:

$$DF_2(X) = \begin{bmatrix} -\gamma(y_1) - f + a_1\alpha_1 & \rho - 2a(y_1 - b)x_1 & 0 & 0 \\ f & -h & 0 & 0 \\ a_1\alpha_0 \frac{-\beta_1 e^{-d_1/l}}{w_0} x_2 & a_1\alpha_0 \frac{-\beta_2 e^{-d_1/l}}{w_0} x_2 & -\gamma(y_2) - f + a_1\alpha_2 & \rho - 2a(y_2 - b)x_2 \\ 0 & 0 & f & -h \end{bmatrix}.$$

Its block triangular shape is due to the master-slave structure of problem (15), thus it can be written

$$DF_2(X) = \begin{bmatrix} J_1(x_1, y_1) & 0 \\ J^* & J_2(X) \end{bmatrix},$$

with

$$J_1(x_1, y_1) = \begin{bmatrix} -\gamma(y_1) - f + a_1\alpha_1 & \rho - 2a(y_1 - b)x_1 \\ f & -h \end{bmatrix},$$

$$J_2(X) = \begin{bmatrix} -\gamma(y_2) - f + a_1\alpha_2 & \rho - 2a(y_2 - b)x_2 \\ f & -h \end{bmatrix},$$

and J^* has not to be specified, since the eigenvalues of $DF_2(X)$ are given by those of $J_1(x_1, y_1)$ and of $J_2(X)$.

Let us first determine the eigenvalues of $J_1(x_1, y_1)$. We have

$$J_1(0, 0) = \begin{bmatrix} -ab^2 - c - f + a_1\alpha_1 & \rho \\ f & -h \end{bmatrix}.$$

Its determinant and trace are given by

$$\det J_1(0, 0) = ah(b^2 - k), \quad \text{tr} J_1(0, 0) = a(k - b^2) - \frac{\rho f}{h} - h.$$

Under the assumption $b > \sqrt{k}$, we obtain $\det J_1(0, 0) > 0$ and $\text{tr} J_1(0, 0) < 0$, which proves that $J_1(0, 0)$ admits two negative eigenvalues. Similarly, we compute $J_1(\bar{x}_1, \bar{y}_1)$. Its determinant is given by

$$\det J_1(\bar{x}_1, \bar{y}_1) = -2a\sqrt{k}(b - \sqrt{k}) < 0,$$

which proves that $J_1(\bar{x}_1, \bar{y}_1)$ admits one positive eigenvalue and one negative eigenvalue. Finally, the determinant and the trace of $J_1(x_1^*, y_1^*)$ satisfy

$$\det J_1(x_1^*, y_1^*) = 2a\sqrt{k}(b + \sqrt{k}) > 0, \quad \text{tr} J_1(x_1^*, y_1^*) = -\frac{\rho f}{h} - h < 0,$$

which proves that $J_1(x_1^*, y_1^*)$ admits two negative eigenvalues.

Following the same method, we determine the eigenvalues of $J_2(X)$. We first compute $J_2(0, 0, 0, 0)$, its determinant and its trace. We have

$$J_2(0, 0, 0, 0) = \begin{bmatrix} -ab^2 - c - f + a_1\alpha_2(0, 0) & \rho \\ f & -h \end{bmatrix},$$

$$\det J_2(0, 0, 0, 0) = ah(b^2 - k) - ah\delta_0 \geq ah(b^2 - k) > 0,$$

$$\text{tr} J_2(0, 0, 0, 0) = a(k - b^2) - \frac{\rho f}{h} - h + a\delta_0 < 0,$$

since $\delta_0 \leq 0$. It follows that $J_2(0, 0, 0, 0)$ admits two negative eigenvalues. Combined with the fact that $J_1(0, 0)$ also admits two negative eigenvalues, it is seen that $E_1 = (0, 0, 0, 0)$ is an attractive node and thus is locally asymptotically stable. We evaluate analogously the jacobian matrix at other equilibrium points. \square

3.3. Bifurcation diagrams and phase portraits

The research of the equilibrium points in the two forests complex network given by system (15) reveals bifurcations processes with respect to a variation of multiple parameters involved in the network problem. We present in Figure 6 three bifurcation diagrams which have been computed with the parameters values given in Table 3. As usual, we depict in continuous lines the stable equilibrium points and in dashed lines the unstable equilibrium points.

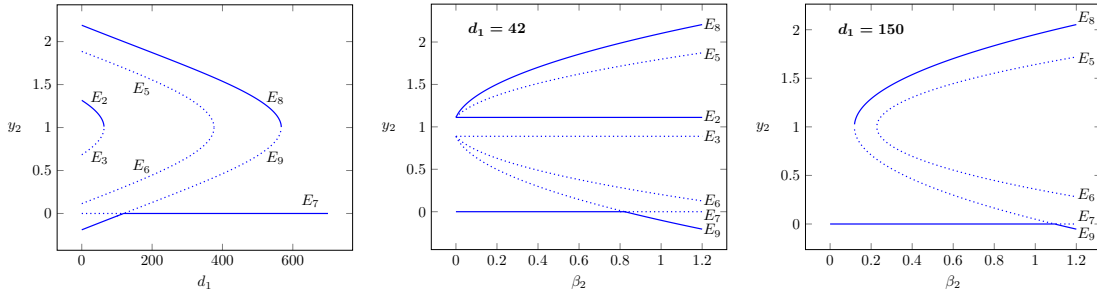


Figure 6: Bifurcation diagrams showing the equilibrium points of the two forest complex network given by (15). Left: an increase of the parameter d_1 , which represents the distance between the two forest ecosystems, leads to two saddle-node bifurcations and one trans-critical bifurcation. Center: an increase of the parameter β_2 involved in the biotic pump mechanism (see equation (4)), with a small value of d_1 , implies that the system exhibits all the possible equilibrium states. Right: with a greater value of d_1 , the complex network is likely to admit only trivial equilibrium states; however, an increase of β_2 allows to recover non-trivial equilibrium points.

In the first bifurcation diagram (Figure 6, left), we consider a variation of the parameter d_1 which models the distance between the two forest ecosystems and we represent the numerical value of y_2 , which corresponds to the fourth coordinate of the equilibrium points given in Table 2. If d_1 is small, then it is seen that the complex network admits 9 equilibrium points. Among those 9 equilibrium

Table 3: Parameters values of the two forest complex network given by (15) chosen for the computation of the bifurcation diagrams presented in Figure 6 and the phase portraits depicted in Figure 7.

Parameter	Value	Parameter	Value
ρ	4.2	a_2	0
f	1	l	600
h	2	P_0	1
a, b, c, w_0	1	β_1	0
α_0	-1	β_2	1
a_1	1	d_1	42, 150, 700

points, the system admits two non-trivial locally stable nodes E_2 and E_8 which attract the orbits and guaranty that the second forest ecosystem reaches a good health equilibrium. In parallel, the equilibrium point E_7 is seen to be unstable (note that we do not represent E_1 nor E_4 in this bifurcation diagram, since they would be superposed with E_7 and hide its change of stability). If d_1 increases, then the complex network exhibits a first saddle-node bifurcation which implies that E_2 vanishes. If d_1 keeps increasing, then the system presents a trans-critical bifurcation since E_7 and E_9 cross and change their stability. This implies that the equilibrium point E_7 becomes attractive, which is likely to attract the orbits of the complex network to an extinction state of the second forest ecosystem. At this stage, E_7 appears to coexist with E_8 which is an attractive node and guarantees a good health equilibrium of the second forest ecosystem. Finally, if d_1 increases again, then the system exhibits a second saddle-node bifurcation which implies that the non-trivial attractive node E_8 vanishes. Thus E_7 and E_1 remain the only attractive equilibrium points, which means that the second forest ecosystem converges to an extinction state. Roughly speaking, if the distance between the two forest ecosystems increases, then the second forest ecosystem is likely to receive a lower quantity of water resource, which is due to the exponentially decrease of the water quantity with the distance; in that case, the good health of the second forest ecosystem may be compromised.

In the two other bifurcation diagrams (Figure 6, center and right), we experiment an increase of the parameter β_2 involved in the biotic pump mechanism (see equation (4)), for two distinct values of d_1 ($d_1 = 42$ in the center diagram, $d_1 = 150$ on the right diagram). An increase of the parameter β_2 means that the capacity of a given forest ecosystem to produce water also increases. With a small value of d_1 , it is seen that the system exhibits all the possible equilibrium states. With a greater value of d_1 , the complex network is likely to admit only trivial equilibrium states; however, an increase of β_2 allows to recover non-trivial equilibrium points. This might suggest the existence of a compensation phenomenon of the distance separating the two forest ecosystems by the efficiency of the biotic pump.

Several phase portraits of the two forest complex network given by (15) are shown in Figure 7 in order to complete the bifurcation diagrams. Those phase portraits have been computed with the same parameters values (see Table 3) and projected in the (x_1, y_1) plane so as to visualize the dynamics of the first ecosystem or in the (x_2, y_2) plane so as to visualize the dynamics of the second forest ecosystem. Initial data have been randomly chosen in $[0, 4]^4$.

The first phase portrait (green orbits) shows the coexistence of three equilibrium points e_1, e_2 and e_3 for the sub-system corresponding to the dynamics of the first forest ecosystem (given by the two first equations in system (15)). The stable equilibrium points e_1 and e_3 admit basins of attraction which are separated by the stable manifold of the saddle-point e_2 . The equilibrium point e_1 corresponds to the convergence of the orbits to an extinction state of the forest ecosystem, whereas the equilibrium point e_3 represents the convergence towards a good health state of the forest ecosystem. The three other phase portraits show the dynamics of the second forest ecosystem (red orbits) for three distinct values of the parameter d_1 which models the distance between the two forest ecosystems. For $d_1 = 42$, the phase portrait exhibits the coexistence of three stable equilibrium points. Among them, E_2 and E_8 attract the orbits to a good health state. For $d_1 = 150$, the attractive equilibrium point E_2 has

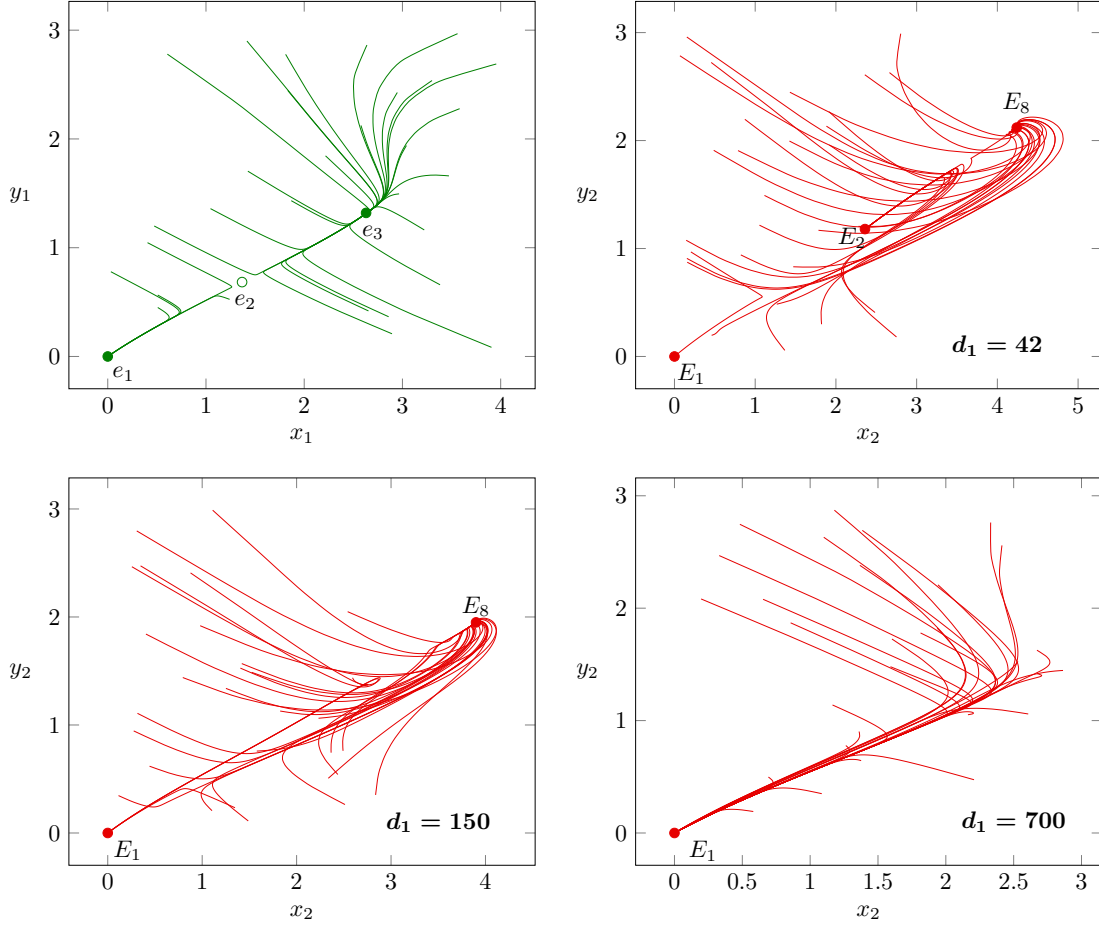


Figure 7: Several phase portraits of the two forest complex network given by (15), projected in the (x_1, y_1) plane so as to visualize the dynamics of the first ecosystem (green orbits) or in the (x_2, y_2) plane so as to visualize the dynamics of the second forest ecosystem (red orbits). Initial data have been randomly chosen in $[0, 4]^4$.

vanished and E_8 remains the only non-trivial stable equilibrium point. Finally, for $d_1 = 700$, all the non-trivial stable equilibrium points have vanished, which implies that the orbits are attracted to the trivial equilibrium which means an extinction state of the second forest ecosystem. Once again, the distance d_1 separating the two forest ecosystems is seen to play a crucial role on the dynamics of the second forest ecosystem.

§4. Sensitivity analysis of the multiple forest ecosystems network

In this section, our aim is to investigate the dynamics of the multiple forest ecosystems network given by system (10). We experiment the impact of an increase of the number of forest ecosystems and discover the emergence of synchronization in the network, which corresponds to the convergence of each ecosystem to a good health state. Then we improve our complex network model by incorporating a randomly generated perturbation which models deforestation. Our numerical simulations have been performed with the `python` language, in a Debian/GNU-Linux environment.

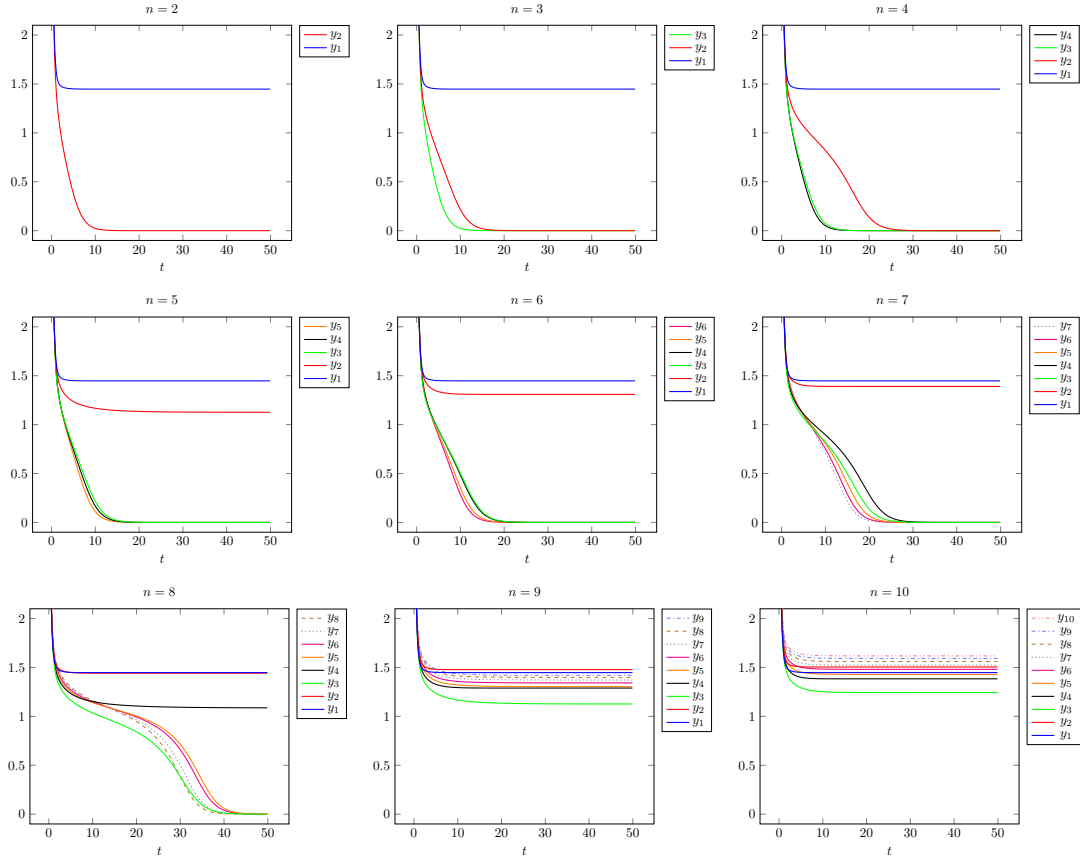


Figure 8: Time series $(t, y_i(t))$ ($1 \leq i \leq n$) of the populations of old trees in each ecosystem of a n forests network of the form (10), obtained for $n \in \{2, 3, \dots, 10\}$. A low number of forest ecosystems leads to the extinction of a part of the network, whereas a sufficiently large number of ecosystems guarantees the synchronization of each ecosystem to a good health state.

4.1. Numerical simulations of the complex network model

The research of the equilibrium states in a two forest ecosystems network has revealed the possible coexistence of 9 equilibrium points. Analogously, it is easy to show that a n forest ecosystems network can admit up to 3^n equilibrium points. Furthermore, the distances separating each forest ecosystem are likely to make non-trivial attractive nodes vanish. Thus it is natural to ask if there exists a distance threshold under which a complex network of forest ecosystems converges to a global good health state.

Let us consider a fix distance $D > 0$ and an integer $n \geq 2$. We set $d = \frac{D}{n-1}$ and we construct a n forest ecosystems network of the form (10), in which the distances between two forest ecosystems are uniformly equal to d . We already know from the previous section the behavior of the network for $n = 2$. In particular, it has been proved that the second forest ecosystem will converge to an extinction state equilibrium if D is sufficiently large. Now we wonder if an increase of n could contrary this process which leads to an extinction state of the ecosystem. In other words, we suppose that intermediate forest ecosystems are implanted between the first forest, which is located nearby the coastline, and the last forest ecosystem, which is located at a distance from the first one equal to D . We present in Figure 8 several time series $(t, y_i(t))$ ($1 \leq i \leq n$) of the populations of old trees in each forest ecosystem, obtained for $n \in \{2, 3, \dots, 10\}$. The parameters values are once again those given in Table 3, except $P_0 = 1.1$, $\beta_2 = 0.3$. Furthermore, we have fixed $D = 1000$.

We observe a change of the dynamics of the network at $n = 9$. Indeed, for $n < 9$, it is seen that at least one forest ecosystem is attracted to an extinction state. For instance, for $n = 4$, we observe that 3 forest ecosystems are attracted to an extinction state and the first forest ecosystem, which is located

nearby the coastline, is the only one to survive. Next, for $n \geq 5$, it is remarked that at least a second forest ecosystem survives. Finally, for $n \geq 9$, the network exhibits the convergence to a non-trivial equilibrium for each forest ecosystem. This common convergence can be seen as a synchronization of each ecosystem in the network to a good health state.

4.2. Random perturbation of the complex network problem

Here we aim to improve our complex network model (10) by incorporating a perturbation modeling deforestation. The causes of deforestation can have various origins. Anthropogenic cause of deforestation is admitted as an obvious fact and discussed in [1] for instance. However, the proliferation of big herbivores is also suspected to have caused deforestation in past periods, implying a cascade of climatic effects, including biotic pump disruption and generally continental climate destabilization (see [6] for instance).

As previously, we fix a distance $D > 0$ and an integer $n \geq 2$. We set $d = \frac{D}{n-1}$ and consider a n forests complex network of the form (10) in which $d_i = d$ for each $i \in \{1, \dots, n\}$. We assume that this complex network problem admits a stable equilibrium $X^* = (x_1^*, y_1^*, \dots, x_n^*, y_n^*)$ with positive components, corresponding to a good health state of each ecosystem of the network, and we consider the equilibrium solution $X(t) \equiv X^*$. The existence of such an equilibrium has been verified in the previous section for a particular value of n .

Now we generate a random integer N such that $0 \leq N \leq n$, and a random list of N distinct integers i_1, \dots, i_N such that $1 \leq i_k \leq n$ for each $k \in \{1, \dots, N\}$. The random list $L = \{i_1, \dots, i_N\}$ models the deforestation of N ecosystems among the n forests which compose the network under study. In parallel, we generate N positive times t_1, \dots, t_N that we associate to the integers i_1, \dots, i_N respectively. The list

$$\{(i_1, t_1), \dots, (i_N, t_N)\} \quad (17)$$

models the choice of N ecosystems which are assumed to be deforested at times t_1, \dots, t_N respectively. Furthermore, we introduce the function $\theta(t, t^*)$ defined by

$$\theta(t, t^*) = \begin{cases} 0 & \text{if } t \leq t^*, \\ \frac{1}{2} - \frac{1}{2} \cos(\pi(t - t^*)) & \text{if } t^* < t < t^* + 1, \\ 1 & \text{else,} \end{cases} \quad (18)$$

in order to model the beginning of the deforestation process at time t^* of a given ecosystem in the complex network. We also introduce the boolean integer ε_k defined by

$$\varepsilon_k = \begin{cases} 1 & \text{if } k \in \{i_1, \dots, i_N\}, \\ 0 & \text{if } k \notin \{i_1, \dots, i_N\}. \end{cases} \quad (19)$$

Finally we consider the randomly perturbed complex network problem defined by

$$\begin{cases} \dot{\tilde{x}}_1 = \rho \tilde{y}_1 - \gamma(\tilde{y}_1) \tilde{x}_1 - f \tilde{x}_1 + a_1 \alpha_1 \tilde{x}_1 - \varepsilon_1 \theta(t, t_1) \tilde{x}_1 \\ \dot{\tilde{y}}_1 = f \tilde{x}_1 - h \tilde{y}_1 + a_2 \alpha_1 \tilde{y}_1 - \varepsilon_1 \theta(t, t_1) \tilde{y}_1, \\ \dot{\tilde{x}}_2 = \rho \tilde{y}_2 - \gamma(\tilde{y}_2) \tilde{x}_2 - f \tilde{x}_2 + a_1 \alpha_2(\tilde{x}_1, \tilde{y}_1) \tilde{x}_2 - \varepsilon_2 \theta(t, t_2) \tilde{x}_2 \\ \dot{\tilde{y}}_2 = f \tilde{x}_2 - h \tilde{y}_2 + a_2 \alpha_2(\tilde{x}_1, \tilde{y}_1) \tilde{y}_2 - \varepsilon_2 \theta(t, t_2) \tilde{y}_2, \\ \vdots \\ \dot{\tilde{x}}_n = \rho \tilde{y}_n - \gamma(\tilde{y}_n) \tilde{x}_n - f \tilde{x}_n + a_1 \alpha_n(\tilde{x}_1, \tilde{y}_1, \dots, \tilde{x}_{n-1}, \tilde{y}_{n-1}) \tilde{x}_n - \varepsilon_n \theta(t, t_n) \tilde{x}_n \\ \dot{\tilde{y}}_n = f \tilde{x}_n - h \tilde{y}_n + a_2 \alpha_n(\tilde{x}_1, \tilde{y}_1, \dots, \tilde{x}_{n-1}, \tilde{y}_{n-1}) \tilde{y}_n - \varepsilon_n \theta(t, t_n) \tilde{y}_n, \end{cases} \quad (20)$$

and we denote $\tilde{X} = (\tilde{x}_1, \tilde{y}_1, \dots, \tilde{x}_n, \tilde{y}_n)^T$. Note that system (20) is non-linear and non-autonomous, whereas system (10) is only non-linear. The following theorem guarantees that the resulting Cauchy problem is well-posed. Its proof can be made by repeating the same arguments as for Theorems 1 and 2, so we skip it.

Theorem 4. Assume that $X^* = (x_1^*, y_1^*, \dots, x_n^*, y_n^*)$ is a non trivial equilibrium point of the complex network (10). Assume furthermore that a_2 is sufficiently small. Then for any randomly generated list $\{(i_1, t_1), \dots, (i_N, t_N)\}$ of type (17), the Cauchy problem defined by (20) and $\tilde{X}(0) = X^*$ admits a unique global solution $\tilde{X}(t, X^*)$, defined on $[0, \infty)$, admitting non-negative components.

4.3. Numerical simulations of the randomly perturbed complex network

Here, we present a selection of numerical simulations of the randomly perturbed complex network (20). We experiment the impact of the level of deforestation on the global dynamics of the complex network. To this end, we distinguish the number N of deforested ecosystems, N being the cardinal of the list $\{(i_1, t_1), \dots, (i_N, t_N)\}$ given by (17), and the number K of killed forests after the deforestation process. We can measure the number K of killed forests by enumerating the indices $i \in \{1, \dots, n\}$ such that

$$\limsup_{t \rightarrow \infty} (x_i^2(t) + y_i^2(t)) = 0.$$

In particular, we investigate the effect of the positions of the deforested ecosystems on the number K of killed forests.

First, we show in Figure 9 the results of four numerical simulations of the randomly perturbed complex network (20).

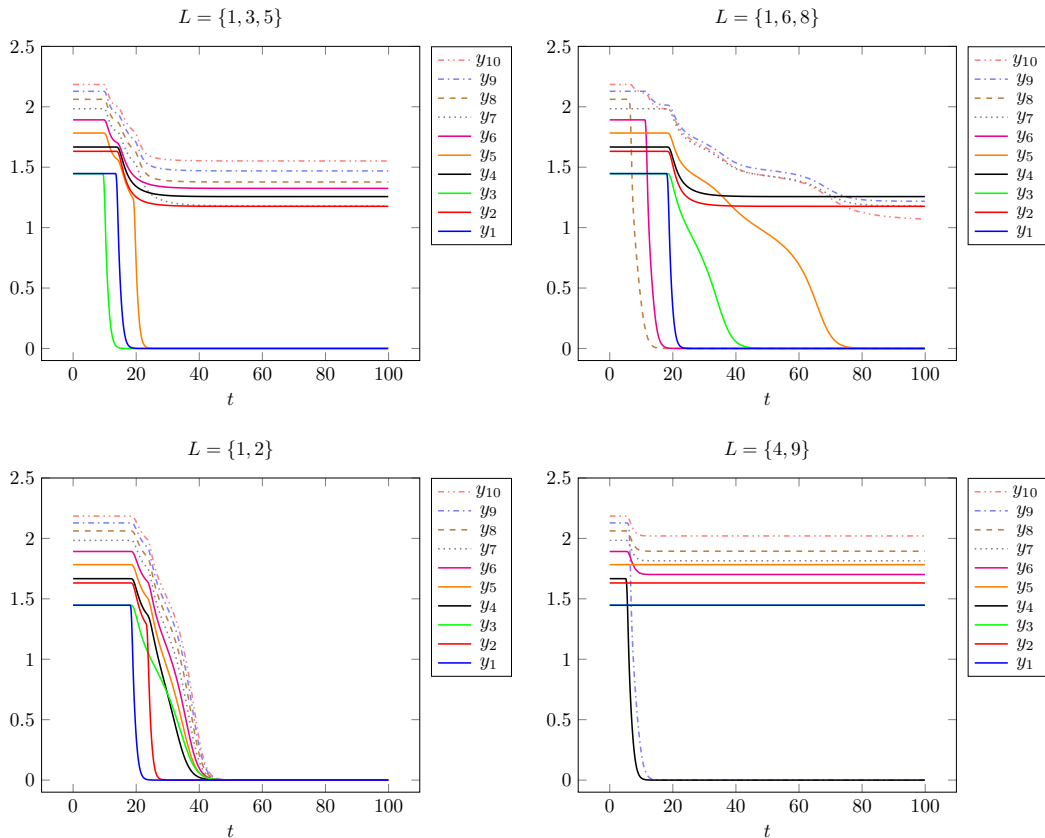


Figure 9: Numerical simulations of the randomly perturbed complex network (20). The positions of the N deforested ecosystems affects the number K of resulting killed forests and tests the level of resilience of the network.

We consider again the case $n = 10$ and $D = 1000$. The values of other parameters are the same as in Table 3. When $L = \{1, 3, 5\}$, thus $N = 3$, we observe that the number of killed forests is also $K = 3$, which means that the complex network exhibits a sort of resilience. This resilience is also observed

when $L = \{4, 9\}$, since we have $K = N = 2$ in this case. However, the resilience is compromised when $L = \{1, 6, 8\}$, since the number of killed forests is now $K = 5$. The consequences of deforestation are drastic when $L = \{1, 2\}$, since each forest ecosystem is killed, that is $K = 10$. This series of random simulations already proves that the location of deforested ecosystems is a key factor of the resilience of the complex network. The values of the delays t_1, \dots, t_N seem to vary the transitional dynamics of the solutions, without changing its asymptotic phase. In other words, the behavior of the complex network seems to be robust to a variation of the times at which the deforestation acts.

Next, we experiment further the level of resilience of the network by computing the number K of killed forests with respect to the positions of the deforested ecosystems, in the cases $N = 1$ and $N = 2$ (see Table 4). We observe an acceptable level of resilience of the network in the case $N = 1$: indeed, the deforestation of a unique ecosystem causes the extinction of at most 3 forests in the network. We also note that the deforestation of the first ecosystem is the most severe. The case $N = 2$ reveals a high sensitivity of the complex network with respect to the locations of the deforested ecosystems, since the deforestation of the two first ecosystems, that is $L = \{1, 2\}$, causes the extinction of the whole network, whereas the deforestation of two ecosystems which are located near the end of the chain (*e.g.* $L = \{6, 8\}$) do not cause more killed forests, that is $K = N = 2$. Those results suggest that the most severe deforestation is obtained when selecting forests which are located nearby the coastline.

Table 4: Impact of the positions in the network of the deforested ecosystems on the number K of killed forests.

N	Positions of the deforested ecosystems	Number K of killed forests
1	$L = \{1\}$	3
1	$L = \{i\}$ with $2 \leq i \leq 10$	1
2	$L = \{1, 2\}$	10
2	$L = \{1, 4\}$	9
2	$L = \{2, 3\}$	8
2	$L = \{1, 6\}$	4
2	$L = \{1, 7\}$	4
2	$L = \{1, 8\}$	4
2	$L = \{1, 9\}$	4
2	$L = \{1, 10\}$	4
2	$L = \{1, 3\}$	3
2	$L = \{1, 5\}$	3
2	Other positions	2

We end our paper with the result of 2000 simulations of the randomly perturbed complex network (20). For each simulation, we compute and compare the number N of deforested ecosystems and the number K of killed forests. Moreover, we enumerate the cases for which the values of N and K coincide. This approach leads to the chart depicted in Figure 10. The horizontal axis represents the number N of deforested ecosystems, whereas the vertical axis gives the number K of killed forests. For each position (N, K) , the size of the disk located at (N, K) represents the number of simulations with output (N, K) among the 2000 simulations. This size can also be recovered with the colorbar. First, we observe that the number of killed forests is always greater than or equal to the number of deforested ecosystems, which follows directly from the construction of the complex network problem (20). But we observe that the gap between N and K increases with N . In other words, if the intensity of deforestation increases, then its consequences are exacerbated. In particular, the whole network can be led to a global extinction state when $N \geq 2$, and the frequency of global extinction states becomes major for $N \geq 6$.

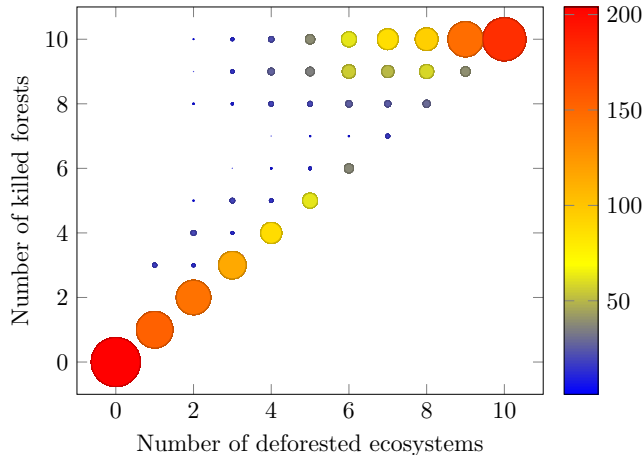


Figure 10: Chart showing the results of 2000 simulations of the randomly perturbed complex network (20). The horizontal axis represents the number N of deforested ecosystems, whereas the vertical axis gives the number K of killed forests. For each position (N, K) , the size of the disk located at (N, K) represents the number of simulations with output (N, K) among the 2000 simulations.

§5. Conclusion

In this article, we have proposed an original mathematical model for studying the dynamics of complex forest ecosystems, which takes into account the biotic pump mechanism and reproduces the principle of constant precipitation quantity over densely forested areas. We have proved the well-posedness of our model, by showing the existence of relevant solutions, and we have performed a stability and bifurcation analysis, from which a main trend emerges: if the distance separating to forest ecosystems increases, then at least one of those ecosystems is likely to converge to an extinction state. Various numerical simulations of our complex network model show the impacts of deforestation and reforestation. The fine calibration of our model will be presented in a separate paper.

In a future work, we aim to improve our model into two directions. First, we aim to consider a bi-dimensional forested area rather than a simplified distribution of forest ecosystems along a single line. The second direction of improvement would correspond to modeling a continuous forest area, using a reaction-advection-diffusion model.

References

- [1] A. A. Alencar, P. M. Brando, G. P. Asner, and F. E. Putz. Landscape fragmentation, severe drought, and the new Amazon forest fire regime. *Ecological applications*, 25(6):1493–1505, 2015.
- [2] A. Alexandridis, D. Vakalis, C. I. Siettos, and G. V. Bafas. A cellular automata model for forest fire spread prediction: The case of the wildfire that swept through spetses island in 1990. *Applied Mathematics and Computation*, 204(1):191–201, 2008.
- [3] M. Y. Antonovsky, R. Fleming, Y. A. Kuznetsov, and W. Clark. Forest-pest interaction dynamics: the simplest mathematical models. *Theoretical Population Biology*, 37(2):343–367, 1990.
- [4] G. Cantin. Non identical coupled networks with a geographical model for human behaviors during catastrophic events. *International Journal of Bifurcation and Chaos*, 2017.
- [5] G. Cantin and J. Silva. Influence of the topology on the dynamics of a complex network of HIV/AIDS epidemic models. *AIMS Mathematics*, 4:1145, 2019.
- [6] V. G. Gorshkov and A. M. Makarieva. Key ecological parameters of immotile versus locomotive life. *bioRxiv*, 2019.
- [7] J. M. Hett and O. L. Loucks. Age structure models of balsam fir and eastern hemlock. *The Journal of Ecology*, pages 1029–1044, 1976.

- [8] J. Hizanidis, V. G. Kanas, A. Bezerianos, and T. Bountis. Chimera states in networks of nonlocally coupled Hindmarsh–Rose neuron models. *International Journal of Bifurcation and Chaos*, 24(03):1450030, 2014.
- [9] M. Hope. Australia burning. *The Lancet Planetary Health*, 4(1):e12–e13, 2020.
- [10] I. Karafyllidis and A. Thanailakis. A model for predicting forest fire spreading using cellular automata. *Ecological Modelling*, 99(1):87–97, 1997.
- [11] F. Kelliher, J. Lloyd, A. Arneth, J. Byers, T. McSeveny, I. Milukova, S. Grigoriev, M. Panfyorov, A. Sogatchev, A. Varlargin, et al. Evaporation from a central siberian pine forest. *Journal of Hydrology*, 205(3-4):279–296, 1998.
- [12] J. P. H. Kimmins, J. A. Blanco, B. Seely, C. Welham, and K. Scoullar. Complexity in modelling forest ecosystems: How much is enough? *Forest Ecology and Management*, 256(10):1646–1658, 2008.
- [13] T. Kohyama. Size-structured multi-species model of rain forest trees. *Functional Ecology*, pages 206–212, 1992.
- [14] Y. Kuznetsov. *Elements of Applied Bifurcation Theory*. Applied Mathematical Sciences. Springer New York, 2004.
- [15] Y. Kuznetsov, M. Antonovsky, V. Biktashev, and E. Aponina. A cross-diffusion model of forest boundary dynamics. *Journal of Mathematical Biology*, 32(3):219–232, 1994.
- [16] P. Magal and Z. Zhang. Competition for light in forest population dynamics: from computer simulator to mathematical model. *Journal of theoretical biology*, 419:290–304, 2017.
- [17] A. M. Makarieva and V. G. Gorshkov. Biotic pump of atmospheric moisture as driver of the hydrological cycle on land. *Hydrology and Earth System Sciences Discussions*, 3(4):2621–2673, 2006.
- [18] V. Méndez and J. E. Llebot. Hyperbolic reaction-diffusion equations for a forest fire model. *Physical Review E*, 56(6):6557, 1997.
- [19] B. Mertens and E. F. Lambin. Spatial modelling of deforestation in southern cameroon: spatial disaggregation of diverse deforestation processes. *Applied Geography*, 17(2):143–162, 1997.
- [20] D. C. Nepstad, C. M. Stickler, B. S. Filho, and F. Merry. Interactions among Amazon land use, forests and climate: prospects for a near-term forest tipping point. *Philosophical Transactions of the Royal Society B: Biological Sciences*, 363(1498):1737–1746, 2008.
- [21] H. G. Othmer, F. R. Adler, M. A. Lewis, and J. C. Dallon. *Case Studies in Mathematical Modeling—ecology, Physiology, and Cell Biology*. Prentice Hall Englewood Cliffs, NJ, 1997.
- [22] E. Pastor, L. Zárata, E. Planas, and J. Arnaldos. Mathematical models and calculation systems for the study of wildland fire behaviour. *Progress in Energy and Combustion Science*, 29(2):139–153, 2003.
- [23] L. Perko. *Differential equations and dynamical systems*. Springer, New York, 3rd edition, 2001.
- [24] V. Perminov. Mathematical modeling of crown forest fires initiation. In *International Conference on Computational Science and Its Applications*, pages 549–557. Springer, 2003.
- [25] S. Qureshi and A. Yusuf. Mathematical modeling for the impacts of deforestation on wildlife species using Caputo differential operator. *Chaos, Solitons & Fractals*, 126:32–40, 2019.
- [26] H. L. Smith and H. R. Thieme. *Dynamical systems and population persistence*, volume 118. American Mathematical Soc., 2011.
- [27] J. Stewart. Evaporation from the wet canopy of a pine forest. *Water Resources Research*, 13(6):915–921, 1977.
- [28] C. Willmott and S. Webber. LBA regional climate data, 0.5-degree grid, 1960-1990. *ORNL DAAC*, 2003.
- [29] S. Zhu, N. Verdière, L. Denis-Vidal, and D. Kateb. Identifiability analysis and parameter estimation of a chikungunya model in a spatially continuous domain. *Ecological complexity*, 34:80–88, 2018.